Improving modelled albedo over the Greenland ice sheet through parameter optimisation and MODIS snow albedo retrievals

Nina Raoult[1], Sylvie Charbit[1], Christophe Dumas[1], Fabienne Maignan[1], Catherine Ottlé[1], and Vladislav Bastrikov[2]

[1]Laboratoire des Sciences du Climat et de l'Environnement, LSCE/IPSL, CEA-CNRS-UVSQ, Université Paris-Saclay, Gif-sur-Yvette, France
[2]Science Partners, Paris, France

Correspondence: Nina Raoult (nina.raoult@lsce.ipsl.fr)

Abstract. Greenland ice sheet mass loss continues to accelerate as global temperatures increase. The surface albedo of the ice sheet determines the amount of absorbed solar energy, which is a key factor in driving surface snow and ice melting. Satellite retrieved snow albedo allows us to compare and optimise modelled albedo over the entirety of the ice sheet. We optimise the parameters of the albedo scheme in the ORCHIDEE land surface model for three random years taken over the 2000-2017 period and validate over the remaining years. In particular, we want to improve the albedo at the edges of the ice sheet since they correspond to ablation areas and show the greatest variations in runoff and surface mass balance. By giving a larger weight to points at the ice sheet's edge, we improve the model-data fit by reducing the RMSD by over 25% for the whole ice sheet for the summer months. This improvement is consistent for all years, even those not used in the calibration step. We conclude by showing which additional model outputs are impacted by changes to the albedo parameters encouraging future work using multiple data streams for optimisation.

1 Introduction

The melting of the Greenland ice sheet (GrIS) is one of the main contributors to sea-level rise (Frederikse et al., 2020). As global temperatures continue to increase under climate change, further melting and surface mass loss are expected (The IMBIE team, 2020), potentially affecting deep ocean circulation (Hu et al., 2011). Increased warming is also expected to darken the GrIS (Tedesco et al., 2016), decreasing the surface reflectivity (i.e. albedo). This darkening has already been observed over the last decades, driven by: snowmelt, the retreat of the snow line, dust deposition, and algae growth (Cook et al., 2020). Since surface albedo determines the land surface energy balance by controlling the amount of reflected solar (shortwave) radiation, reductions in albedo - through the darkening of the ice sheet - result in increased shortwave absorption. This, in turn, enhances melting, creating a strong feedback to the atmosphere. The melt-albedo feedback is an essential contributor to mass loss (Qu and Hall, 2014; Zeitz et al., 2021) and can be used as an emergent constraint to reduce the inter-model variability in projections of climate change (Thackeray et al., 2021).

Given the importance of albedo, it is crucial that it is accurately simulated in the land surface models (LSMs) used to generate climate change projections. Therefore it is important to confront LSM albedo estimates with observed values. With large areas

such as the GrIS, we can rely on remote sensing-based albedo measurements derived from various polar-orbiting satellites (Qu et al., 2015). We can use these data to evaluate and optimise LSMs using data assimilation.

Data assimilation (DA) refers to the act of incorporating observational information into a model to constrain its estimates or parameters. Several studies have used remotely sensed albedo for DA in LSMs. For example, Malik et al. (2012) used MODIS (Moderate Resolution Imaging Spectroradiometer; Schaaf et al. (2002))-based snow albedo and direct insertion methodology in the Noah LSM over three sites in Colorado to improve simulated snow depth and snow season duration. Satellite-based albedo data was also used by Wang et al. (2015) to calibrate the ORCHIDEE LSM and investigate the impacts of albedo assimilation on offline and coupled model simulations. Navari et al. (2018) used satellite-derived albedo to improve surface mass balance (SMB) estimates from the CROCUS snowpack model along Greenland's Kangerlussuaq transect. Other datasets have also been assimilated to improve snow estimation, including snow cover fraction estimates from optical sensors (e.g., Toure et al., 2018; Xue et al., 2019) and measured ice surface temperatures (e.g., Navari et al., 2018). There have also been several studies assimilating joint datasets. For example, MODIS-based snow cover fraction and albedo have been assimilated in the Common Land Model LSM (Xu and Shu, 2014) and the Noah LSM Kumar et al. (2020). All these studies use DA for state estimation, i.e., updating the model state whilst keeping the model parameters fixed. The techniques used range from relatively simple methods like direct insertion to more advanced statistical techniques like the ensemble Kalman filter and particle filters.

Examples of DA used for parameter estimation, i.e., optimising internal model parameters, in snow modelling are less common. Bonan et al. (2014) demonstrated how DA can be used for joint state and parameter assimilation in ice sheet modelling. Nevertheless, DA for parameter estimation remains more commonly used by the LSM community to optimise vegetation parameters (see orchidas.ipsl.lsce.fr for such examples calibrating the ORCHIDEE LSM). In these types of studies, it is common to optimise over a single site (or single pixel) or a group of individual pixels, usually sharing a common trait (e.g. the dominant vegetation present), in what is known as a "multisite" approach (e.g., Kuppel et al., 2012; Raoult et al., 2016). In each case, the optimisation results in sets of parameters that apply to that individual site or trait tested. These approaches were used because, historically, models were optimised against in situ measurements from sites that are sparsely and unevenly distributed. Advances in satellite data retrieval have helped provide data over large areas for which we previously had no measurements. However, with large amounts of data, computational power and time still limit the experiments we can perform, which is why the multisite approach is common.

Using MODIS snow albedo, in this study, we use DA for parameter estimation to improve the albedo parameterisation inside the ORCHIDEE LSM (Krinner et al., 2005). Instead of using a single or multisite approach which samples the space, here, to exploit the full spatial coverage of the satellite retrievals, we optimise over the whole area of the GrIS to obtain one best set of model parameters applicable over the full ice sheet. Although this study is only over the GrIS, we can apply the method to other regions. We show how robust Bayesian parameter estimation is an important tool for model development. We further highlight the different limitations and considerations needed to apply such an approach.

2 Methods and Data

2.1 ORCHIDEE land surface model

The ORCHIDEE (ORganizing Carbon and Hydrology in Dynamic Ecosystems) land surface model is the terrestrial component of the IPSL Earth system model (ESM) used in climate projections (Boucher et al., 2020; Cheruy et al., 2020). Either run off-line (i.e., driven by prescribed meteorological forcing) or coupled with an atmospheric model (i.e., as part of the ESM), ORCHIDEE describes the exchanges of energy, water, and carbon between the atmosphere and the continental biosphere. The land surfaces are represented as fractions of bare soil and plant functional types. These surfaces can further be covered with snow.

In this study, we adapted the CMIP (Coupled Model Intercomparison Project) 6 version of ORCHIDEE to run over the GrIS. The CMIP6 version of ORCHIDEE uses the three-layered snow model presented in Wang et al. (2013). To apply ORCHIDEE over the GrIS, we implemented a new soil type into this version of ORCHIDEE to mimic the presence of ice in regions defined by the present-day ice mask (Bamber et al., 2013). In ORCHIDEE, each soil type is defined according to the USDA (United States Department of Agriculture) taxonomy, which classifies soils as a function of their chemical, physical and biological properties (Carsel and Parrish, 1988). For the new icy soil type, the porosity and the saturated volumetric water content are set to 0.98 to simulate a soil filled with frozen water. All the other characteristics of this new soil type were set to those of the loam soil type because it is the dominant soil type in the non-ice-free regions around the GrIS (Fischer et al., 2008). Furthermore, to be able to compare directly modelled to satellite retrieved albedo values, we computed the mean of albedo in both visible (VIS) and near-infrared (NIR) spectral domains. We only consider this averaged albedo in the rest of the study.

In the absence of fresh snow, snow-covered albedo in ORCHIDEE (α_{snow}) decreases exponentially with time from its fresh value (A_{aged}+B_{dec}) to a minimum value after ageing, i.e. albedo of old snow (A_{aged}),

$$\alpha_{snow} = \mathbf{A_{aged}} + \mathbf{B_{dec}} \exp\left(-\frac{\tau_{snow}}{\boldsymbol{\tau_{dec}}}\right). \tag{1}$$

Here the B_{dec} and τ_{dec} parameters control the decay rate of snow albedo. This formula can be used to calculate the snow-covered albedo over different vegetation types, with different values of A_{aged} and B_{dec} accounting for the variability of snow coverings. The parameterisation of snow age, τ_{snow}, is shown in Eq. 2,

$$\tau_{snow}(t+dt) = \tau_{snow}(t) + f_{age} \tag{2}$$

where t is the time, dt is the model time step (1800s). The latter term of equation f_{age}, represents the effect of low temperatures on metamorphism,

$$f_{age} = \left[\frac{\left(\tau_{snow}(t) + \left(1 - \frac{\tau_{snow}}{\boldsymbol{\tau_{max}}}\right)\cdot dt\right)\cdot \exp\left(-\frac{P_{snow}}{\boldsymbol{\delta_c}}\right) - \tau_{snow}(t)}{1 + g_{temp}(T_{soil})}\right]; \qquad g_{temp}(T_{soil}) = \left[\frac{\max(T_0 - T_{soil}, 0)}{\boldsymbol{\omega}}\right]^{\boldsymbol{\beta}} \tag{3}$$

where P_{snow} is snowfall, δ_c is the snowfall depth required to reset the age of the snow, τ_{max} is the maximum snow age, T_0 is the melting temperature (0°C), T_{soil} is soil temperature, and ω and β are tuning constants. All the parameters in bold are listed in Table 1. These, along with the albedo of ice, α_{ICE}, are the parameters we focused on in this study.

Table 1. Parameters of the snow model. The default values represent the values used in the standard simulation of ORCHIDEE, min and max refer to the range over which the parameters are allowed to vary during our experiments.

Parameter	Description	Name in code	Default values	Min	Max
A_{aged}	Sum to be the albedo of fresh snow	SNOWA_AGED*	0.62	0.50	0.70
B_{dec}		SNOWA_DEC*	0.169	0.10	0.40
δ_c	Snowfall depth required to reset the snow age (m)	SNOW_TRANS_NOBIO	0.2	0.2	2
τ_{dec}	Snow age decay rate (days)	TCST_SNOWA_NOBIO	10	1	10
ω	Tuning constants for glaciated snow covered areas	OMG1	7	1	7
β		OMG2	4	0.5	4.5
τ_{max}	Maximum snow age	MAX_SNOW_AGE	50	40	60
α_{ICE}	Ice albedo	ALB_ICE	0.4	0.3	0.5

* note the sum of A_{aged} and B_{dec} must be less than or equal to 1 - this constraint is enforced during the optimisations.

2.2 MAR

The ORCHIDEE model was forced using meteorological outputs from the regional climate model Modèle Atmosphérique Régional (MAR; Gallée and Schayes (1994)), version 3.11.4. MAR is a regional atmospheric model that uses 6 hourly ERA-Interim reanalyses data from the European Centre for Medium-Range Weather Forecasts (ECMWF, Dee et al. (2011)) to prescribe the atmospheric boundary conditions outside the domain. Outputs from the MAR have a resolution of 20 km and a 3 hourly time step. In addition to the MAR meteorological outputs, we consider runoff, sublimation and SMB outputs in this study to assess the impact of the optimisation on these simulated quantities.

2.3 MODIS snow albedo

In this study, we used satellite-derived snow albedo from the NASA (National Aeronautics and Space Administration) MODIS (Moderate-Resolution Imaging Spectroradiometer) MOD10A1 product (Hall et al., 1995). This product uses data from the Terra satellite, which has a sun-synchronous, near-polar circular orbit crossing the equator at approximately 10:30 A.M. local time (Hall and Riggs, 2016) and providing global coverage every 1-2 days. MOD10A1 is a clear-sky daily product. When more than one retrieval is available on a given day, which is the case near the poles, the best value is kept. This best value is chosen based on solar elevation, distance from nadir and cell coverage (Hall and Riggs, 2016). In addition, pixels in the MOD10A1 with solar zenith angles greater than 70° are masked (night is defined as a solar zenith angle greater than 85°).

The version of MOD10A1 we used in this study was further processed by Box et al. (2017). Using data from collection 6 of MOD10A1 (Riggs et al., 2015; Hall and Riggs, 2016), Box et al. (2017) de-noised, gap-filled and calibrated the data into a daily 5km grid covering Greenland for the years 2000-2017. This dataset was further validated against ground-based measurements from the PROMICE stations (Fausto et al., 2021) and the residual bias in the dataset based on the solar zenith angle corrected for using a linear regression according to time and latitude (Box et al., 2017). Finally, in this dataset, when there is inadequate

solar illumination to compute the albedo during the winter months (January, February, November, and December), Box et al. (2017)'s distribution swaps in the April values.

In this study, we used the dataset created by (Box et al., 2017), further aggregating these data to the resolution of the ORCHIDEE outputs, imposed by the meteorological forcing files (20 km).

2.4 ORCHIDAS

2.4.1 A Bayesian framework

To perform the optimisations, we used ORCHIDAS, the ORCHIDEE data assimilation system. ORCHIDAS is a variational DA system in which all observations within the assimilation time window are included in the optimisation. It uses a Bayesian statistical formalism (Tarantola, 2005) where errors associated with the parameters, the observations, and the model outputs are assumed to follow Gaussian distributions. The optimal parameter set corresponds to the minimum of a cost function, J($\mathbf{x}$):

$$J(\mathbf{x}) = \frac{1}{2}\left[(\mathbf{y} - M(\mathbf{x}))^T \mathbf{R}^{-1}(\mathbf{y} - M(\mathbf{x})) + (\mathbf{x} - \mathbf{x}_b)^T \mathbf{B}^{-1}(\mathbf{x} - \mathbf{x}_b)\right] \tag{4}$$

where J($\mathbf{x}$) measures the mismatch between (i) the observations y and the corresponding model outputs $M(\mathbf{x})$ (where M is the model operator), and (ii) the a priori ($\mathbf{x}_b$) and optimised parameters ($\mathbf{x}$). Each term is weighted by its error covariance matrices, $\mathbf{R}$ and $\mathbf{B}$. As in most studies, we set both matrices to be diagonal. We defined the observation error (variance) as the mean-squared difference between the observations and the prior model simulation so that this variance reflects not only the measurement errors but also the model errors. This observation error was approximately 0.06 at the edge of the ice sheet to 0.02 in the middle.

To minimise the cost function, two algorithms were considered in this study. They both work by varying the full set of parameters considered within the ranges prescribed, retaining at each iteration the set of parameters which reduces J(x) compared to the previous iteration. The first algorithm is a deterministic gradient-based method that uses the quasi-Newton algorithm L-BFGS-B to iteratively minimise the cost function (limited memory Broyden–Fletcher–Goldfarb–Shanno algorithm with bound constraints; see Byrd et al. (1995)), simply referred to as BFGS. At each iteration of the BFGS algorithm, the cost function is evaluated as well as its gradient with respect to each parameter. The gradient is calculated with a finite-difference approximation, i.e., using the ratio of change in model output against the change in the model parameter value. The algorithm terminates when the cost function no longer decreases, i.e, the relative change in the cost function becomes smaller than 10^{-4} between successive iterations.

The second algorithm considered is a stochastic random search method, the genetic algorithm (GA), which belongs to a larger class of evolutionary algorithms that follows the principles of genetics and natural selection (Goldberg, 1989; Haupt and Haupt, 2004). With each gene corresponding to a different parameter, a vector of parameters is considered to be a chromosome. At each iteration, p chromosomes are created (where p is the population selected by the user, here chosen to be 30). For the first set of chromosomes, the parameters are randomly perturbed. For subsequent iterations, the chromosomes are created from the previous iteration by one of two processes. The first is the "crossover" process. This is the exchange of the gene sequences of

two parent chromosomes. The second process is "mutation", where selected genes of one parent are randomly perturbed. The best p chromosomes are then kept and ranked, based on their cost function values. More weight is then given to the best parents for the next random selection. Further descriptions of both methods can be found in Bastrikov et al. (2018)'s comparative study.

2.4.2 Sensitivity analysis

With ORCHIDAS, it is also possible to perform a sensitivity analysis (SA) of the model. An SA tests the sensitivity of a model output (usually a physical variable). It tests how the output changes, with respect to different inputs - here the model parameters. This is usually done before optimisation to ensure the right parameters and ranges of variation are used in the main experiments. In this study we use the Morris method (Morris, 1991; Campolongo et al., 2007), which is effective with relatively few model runs compared to other methods (e.g., Sobol', Sobol (2001)). Using an ensemble of parameter values, the Morris method determines incremental ratios, known as 'elementary effects', based on changing parameters one at a time in a sequence for many trajectories which populate parameter space. The mean (μ) and standard deviation (σ) of the differences in model outputs for all the trajectories are calculated. This global method determines which parameters have a negligible impact on the model and which have linear and non-linear effects. The results of this method are qualitative, ranking the parameters in order of significance. To assess the results, we look at the normalised means, dividing through by μ of the most sensitive parameter. As such, the values we consider are between 0 and 1, with 1 representing the most sensitive parameters and 0 parameters with no sensitivity. Morris has also been previously used to test parameters for calibration of an earlier version of the ORCHIDEE snow model (Wang et al., 2013; Dantec-Nédélec et al., 2017).

2.4.3 Performance metrics

To assess the optimisation results, we rely on two standard metrics: the root-mean-square deviation (RMSD) and total absolute error (TAE),

$$\text{RMSD} = \sqrt{\frac{\sum_{i=1}^{n}[\mathbf{y}_i - M(\mathbf{x}_i)]^2}{n}}; \qquad \text{TAE} = \sum_{i=1}^{n}|\mathbf{y}_i - M(\mathbf{x}_i)| \tag{5}$$

where n is the total number of data points.

2.5 Experimental setup

2.5.1 Defining edges

The edges of the ice sheet are of particular interest since they correspond to ablation areas and show the greatest variations in runoff and surface mass balance (SMB). To identify the edges of the GrIS, we exploited the fact that the edges are steeper than the middle of the ice sheet. To calculate the slope of a given pixel, we used the NOAA (National Oceanic and Atmospheric Administration) National Geophysical Data Center (NGDC) - ETOPO2 product (NOAA, 2006), which is based on a 2 arc-minute global relief model of Earth's surface and integrates land topography and ocean bathymetry. This product is already integrated into the ORCHIDEE, where it is used to determine the fraction of runoff that pools in flat areas (Ducharne, 2016;

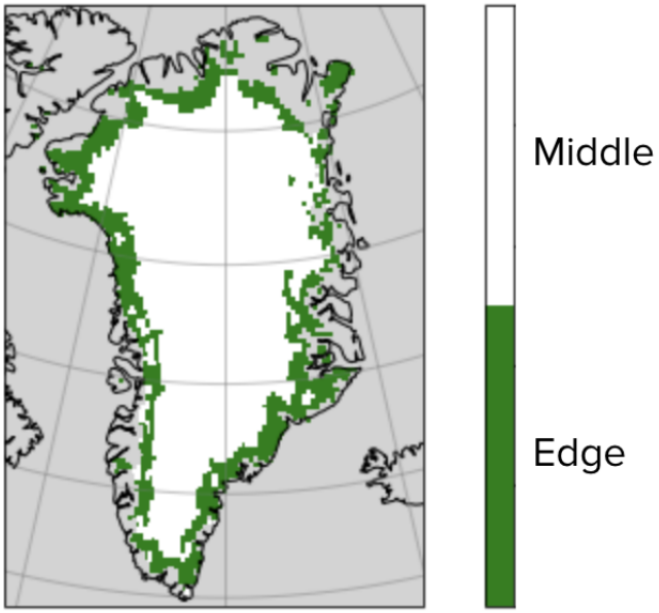

Figure 1. Spatial distribution of edge points (green) and middle points (white); selected based on the steepness of the pixel.

d'Orgeval et al., 2008). In a default ORCHIDEE simulation, when the slope is greater than 0.5%, all precipitation over that pixel that exceed the infiltration capacity is run off immediately (Hortonian runoff) otherwise, it can pond at the soil surface and infiltrate at the next time step. Remember that each pixel in our Greenland simulations in this study has a resolution of 20 km and so the steepness of the slope applies over a large region. We found that by using this same threshold of 0.5%, we were able to encapsulate the edges of the GrIS (Fig. 1). As such, we refer to pixels with a slope gradient greater than 0.5% as "edge" points and the rest as "middle" points. These edge points account for just over 25% of all pixels. They were also the pixels with the largest errors when compared to the retrieved MODIS snow albedo data; these edge pixels represented 78% of the pixels with RMSD greater than 0.1.

2.5.2 Performed experiments

ORCHIDEE was run over the whole GrIS with a spatial resolution of 20 km and a half-hourly time step, with a daily output frequency. The model was driven using meteorological data from MAR and confronted with MODIS albedo retrievals aggregated to the same resolution of 20 km. All the simulations performed in this study include two years of model spin-up to allow the snow to accumulate. These two years are not included in calculating the cost function during the optimisations or during the analysis, but are important in ensuring correct initial states. Furthermore, since during the winter months there is not enough solar illumination to compute the albedo, the months November to February are excluded from the optimisations and analyses.

To begin the study, we performed a sensitivity analysis using Morris's method to understand the relative importance of the different model parameters in simulating albedo. In this experiment, we also considered additional parameters controlling the

rate of density change and additional model outputs including SMB and runoff. These were included to better understand the relationship between different ice sheet processes and to identify which parameters and model output we might consider in future optimisations. This analysis compared ORCHIDEE outputs to the MAR model outputs, testing how each parameter affected the RMSD between both models.

Before the main optimisation, a couple preliminary experiments were performed to select the minimisation algorithm and gauge the maximal improvement we could expect at the edges of the ice sheet, full details of which can be found in the Appendix A. We found that the genetic algorithm greatly outperformed the BFGS algorithm, reducing the cost function by 11% compared to a negligible reduction, and that 15 iterations of the genetic algorithm were sufficient for convergence. We also found that since the number of edge points is being dwarfed by the much denser middle of the ice sheet (see Sect. A), improvements were mainly concentrated over the middle of the ice sheet. This led us to we chose to give extra weight to edge points during the optimisation. The edge points account for approximately a quarter of the points. To ensure the edges and middle both contribute to the cost function, while also giving a bit more focus to the edge points, we chose to give an extra weight of four to the edges when calculating the cost function in the main optimisation.

For the main experiment, to capture the inter-annual variability of snow albedo, we selected three random years to perform our optimisation: 2000, 2010, and 2012. We optimised over these three years simultaneously. This means that, in this main experiment, we minimised a cost function comprising a sum of three cost functions, one for each year considered. The rest of the 2000-2017 time series was used for validation. During this main experiment, we optimised over the whole of the GrIS but gave an extra weight of four to the edge points (see Sect. 2.5.1). This main experiment, referred to as "Both", was complemented by two more optimisations: one just over the edges of the ice sheet ("Edges") and one just over the middle points ("Middle"), again for the same three years. These were done to help analyse the posterior parameter values in Sect. 3.3.2.

3 Results

3.1 Prior model

Before using ORCHIDAS to optimise the model parameters, the ORCHIDEE model was first tuned manually through trial and error. While not as robust as using a Bayesian framework, this initial step is common for land surface modellers and helps get a sense of the different parameter sensitivities. The primary focus of this manual tuning was to better capture the behaviour of the GrIS at its edges. This was achieved by increasing the overall albedo of fresh snow (A_{aged} + B_{dec}) and the snowfall depth required to reset the snow age (δ_c), while also decreasing the albedo of aged snow and decreasing the rate of snow age decay (τ_{dec}). Furthermore, one of the tuning constants for glaciated snow-covered areas was decreased (ω). The rest of the parameters were kept as the default ORCHIDEE parameters (see Table B1 for full results).

This initial tuning helped the model to better simulate the albedo at the edges of the ice sheet, especially in the western part (Fig. 2), as well as other snow states such as SMB and runoff, which were also used to assess the success of the manual tuning. The tuned model was able to capture slightly more the spatial variability of albedo in the middle of the ice sheet.

However, the north-south albedo gradient observed in the satellite retrievals was still not simulated and overall, the albedo remains underestimated over the ice sheet. This initially tuned model was used as the prior for the albedo optimisation.

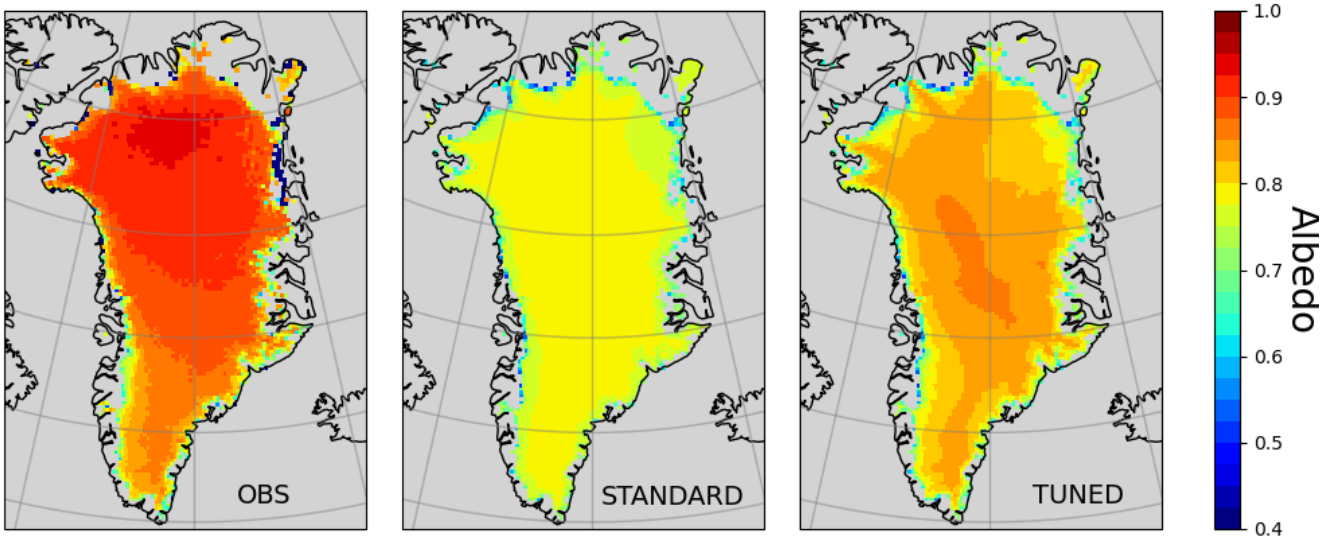

Figure 2. Retrieved and simulated mean albedo over Greenland (averaged over March-October for 2000-2017); the left panel shows the retrieved MODIS values, the middle panel shows simulated albedo in the currently operational ORCHIDEE version and its standard parameter values, and the right panel the simulated albedo from the manually tuned model.

3.2 Sensitivity analysis

In any parameter estimation study, performing a preliminary sensitivity analysis is typical to select the parameters for the optimisation. Since the different processes of the snow model are interlinked, we decided to perform a sensitivity analysis over a range of model outputs to help understand which simulated quantities are also affected by the albedo parameters. In addition to understanding the different sensitivities, this experiment was also done to highlight which further parameterisations to consider in future experiments if we were to optimise the snow model against other types of observations either individually or simultaneously with the albedo retrievals. We add parameters from two other parameterisations controlling snow viscosity and settling of freshly fallen snow (described in Sect. B2) to get a better idea of the relative importance of the different parameters.

Parameters from the albedo parameterisation significantly affect the other simulated outputs tested. For the simulated albedo, the most sensitive parameter is B_{dec} for both the middle and edge of the ice sheet (Fig. 3). We also see that the heat fluxes, surface temperature, and sublimation in the middle of the ice sheet are sensitive to this parameter. In addition, the parameter controlling the snow decay rate (τ_{dec}) is the most sensitive parameter for simulating sublimation and the latent heat flux over the whole ice sheet, and one of the most sensitive for sensible heat flux. Since both B_{dec} and τ_{dec} control the impact of snow

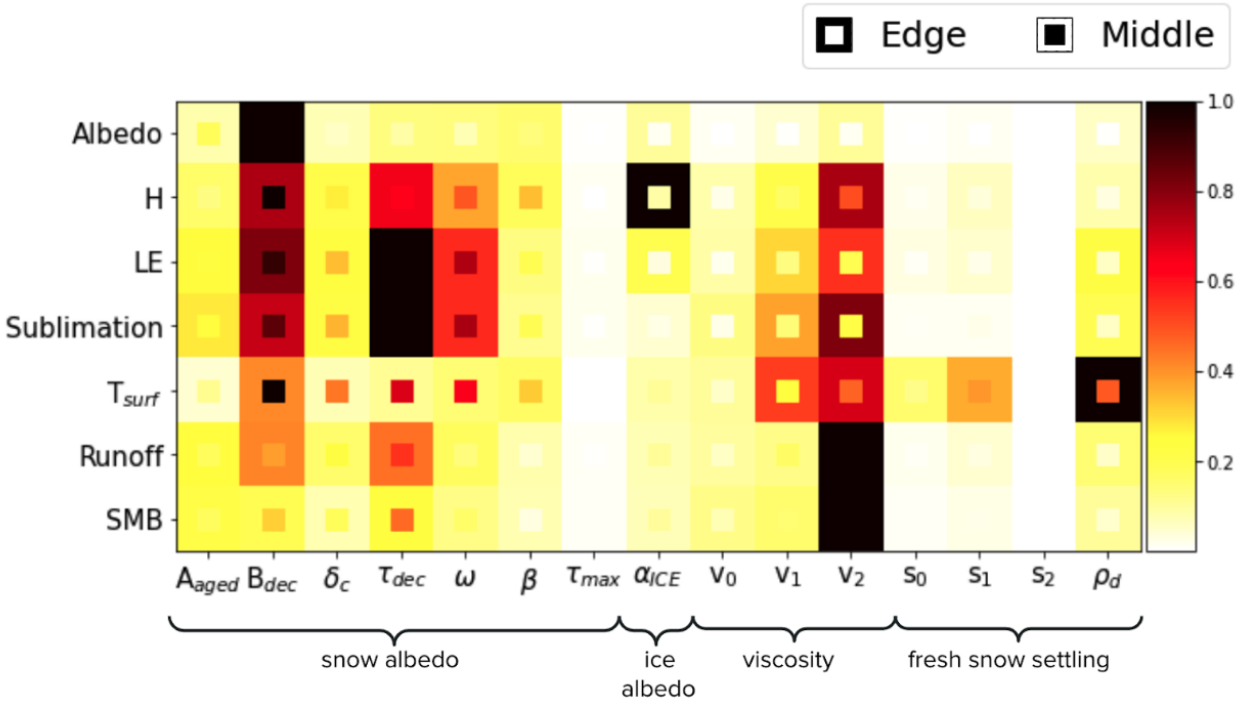

Figure 3. Heatmap showing the relative sensitivity of each parameter for different simulated model outputs; albedo, sensible heat flux (H), latent heat flux (LE), sublimation, surface temperature (T_{surf}), runoff, and surface mass balance (SMB). In each case, the sensitivity of the parameters is shown for simulated quantities at the edge of the ice sheet (shown by the filling at the edge of each box) and in the middle of the ice sheet (shown by the filling in the middle of each box). Morris scores are normalised by the highest ranking parameter in each case. Dark squares represent the most sensitive parameters for each output, and light squares represent parameters with little to no sensitivity.

decay, they directly impact the albedo of the snow and, therefore, the surface temperature. The surface temperature directly affects runoff and the sensible heat flux (calculated as a function of the difference between the surface temperature and the temperature of the atmosphere). The latent heat flux depends directly on the snow, ice and bare soil fractions. The higher the amount of runoff, the more likely it is to have areas where all the snow melts (or grid points where the snow fraction decreases). Therefore the latent heat flux on the snow decreases and so does the sublimation.

The model outputs are only marginally sensitive to τ_{max}. Since we normalise the Morris score by the highest ranking parameter, this shows that compared to the most sensitive parameter, τ_{max} is the least important albedo model parameter in explaining possible range of responses for each modelled output tested. Although seen to be correlated to δ_c at the optimum of the cost function (Fig. 6b), changes in δ_c have more impact on the model outputs than τ_{max}, especially at the centre of the ice sheet. Since δ_c appears in the exponential term of Eq. 2, small variations in its value will have a larger impact on the snow age τ_{snow} than small variations in τ_{max}. Nevertheless, δ_c is the second least sensitive albedo parameter for simulated albedo.

The last two parameters of the albedo parameterisation, ω and β, can be seen to impact temperature and the sensible heat flux at the centre of the ice sheet. These parameters are present in the part of the parameterisation controlling the effect of low temperature on metamorphism (Eq. 3). Since, by influencing snow ageing, these parameters impact surface temperature (through changes in albedo) and thus the sensible heat flux.

The sensible heat flux is especially sensitive to the parameter determining the ice albedo at the edges of the ice sheet. We expect the snow to melt faster at the edges exposing the bare ice below and hence increasing the importance of ice albedo. The ice albedo will therefore impact the surface temperature at these exposed edge points and thus the sensible heat flux.

Modelled albedo is not very sensitive to parameters from the viscosity and fresh snow settling parameterisations - especially not at the centre of the ice sheet. However, these parameters are important for other modelled quantities.

The runoff, surface mass balance, and sublimation are sensitive to the viscosity parameters (Eq. B2), with the parameter controlling the impact of snow density on this parameterisation (v_2) highlighted as the most sensitive. When viscosity decreases, snow density increases and liquid water holding capacity decreases. This leads to an increase in runoff and a decrease in SMB. If the increase in runoff at the edges leads to a significant decrease in snow cover, this will also impact sublimation (which depends on the snow fraction and temperature).

The ice sheet temperature at the surface is sensitive to fresh snow settling parameters (Eq. B3), especially to ρ_d. When considering the rate of density change equation (Eq. B1), we can see it is made up of two terms: a term representing the compaction due to snow load and a term parameterising the effect of metamorphism, which is significant for fresh settling snow. With newly fallen snow, ρ_{snow} is generally low (50-200 kg.m^{-1}), especially in cold environments with little wind. Depending on the value of ρ_d, the density term in Eq. B3 will become zero more or less quickly, maximising the value of ψ_{snow}. This, in turn, increases the density of snow (ρ_{snow}) in the model. As the density of snow increases, the snow becomes less insulating, and the thermal conductivity inside the snowpack increases. In other words, the temperature inside and at the snowpack's surface depends directly on the snow density. This sensitivity to the fresh snow settling parameters may be more important at the edges of the ice sheet because there is more precipitation than in the centre, where the climate is colder and therefore drier.

Although modelled albedo is not very sensitive to parameters from the other parameterisations tested, these parameters greatly impact other model outputs. These model outputs, in turn, are sensitive to these other parameters, especially those from the viscosity parameterisation. Therefore, for future experiments, this sensitivity analysis suggests that to optimise energy budget, runoff and sublimation simultaneously, we would need to consider including the parameters from the albedo and viscosity parameterisations. However, for this study, we only focus on the parameters from the albedo parameterisation (and the albedo of ice) for optimisation since the parameterisation has a manageable number of parameters and the parameter from the other parameterisations show less sensitivity to modelled albedo.

3.3 Main optimisation

3.3.1 Optimisation and validation

For the main optimisation, the GrIS albedo was optimised over the years 2000, 2010 and 2012 simultaneously, with a larger weight given to the edges (see Sect. 2.5.2 for the full setup description). Although a subset of three years was used in this optimisation, the improvement observed is consistent over all years (Figure 4a and Table 2). Indeed, some of the years with the greatest reductions in RMSD were years not used in the optimisation e.g. 2003, 2009, and 2016. We also see that the optimisations improve the fit to the winter months which were not used in the optimisation. When averaged over the whole GrIS, the winter months were seen to be underestimated (Figure 4a). The winter values are still underestimated after optimisation, but much less severely. The troughs during the summer months are where the improvement is the most marked. The albedo during the summer months in prior simulations decreased too much. In the posterior run, these troughs more closely match the retrieved values.

When considering the errors of the posterior model spatially (Figure 4b), we noticed a slight underestimation of modelled albedo in the north of the ice sheet and a slight overestimation in the south. We also see that the edges are mostly overestimated. However, the RMSD reductions over the edge points are similar in magnitude to the reductions found in the preliminary optimisation where only the edge points were considered (Tables A1 and 2). This means that the weighting used between the edge and middle points during the optimisation was sufficient - we have achieved as low RMSD at the edges as in the edge-only experiment. By including the middle points in our optimisation, we greatly improve the fit of the model in the middle of the ice sheet - much more so than when only focusing on the edges (43.7% reduction compared to 8.51%). Figure 5 further illustrates where the error is reduced. By decomposing the TAE, we can see that both the edge and the middle points contribute to the error reduction. This figure also allows us to compare the improvements between the different ORCHIDEE simulations. Note that the tuned model was used as the prior for the optimisation. The optimised model has the lowest error overall, both for the middle and the edges of the ice sheet. This figure highlights the power of the ORCHIDAS approach - the total absolute error is reduced more significantly using the Bayesian framework than when the manual tuning approach was used.

3.3.2 Posterior parameters

In this section, we consider how the parameter values have changed to fix the model-data disparities. In Fig. 6a, we look at the posterior parameters from the main experiment (referred to as "Both") and posterior parameters from experiments solely optimising the edge points ("Edges") and solely optimising the middle points ("Middle"). Initially, the prior model underestimated the albedo. This underestimation is seen both temporally (Fig. 6a), where the maximum simulated albedo is below that of the retrieved values, and spatially (Fig. 2), where the underestimation is most noticeable over the centre of the ice sheet. For all three optimisations, A_{aged} and α_{ICE} increase, contributing to fixing this underestimation. These two parameters directly impact the albedo - as they increase, so will the albedo of the GrIS. We also saw that in the prior model, the albedo decayed too much in summer (Fig. 6a). In the posterior models, the value of the B_{dec} parameter is lowered, giving less weight to the decay term in Eq. 1. Again, this decrease occurs for all three optimisations. Similarly, τ_{dec} increases in all cases, which

a)

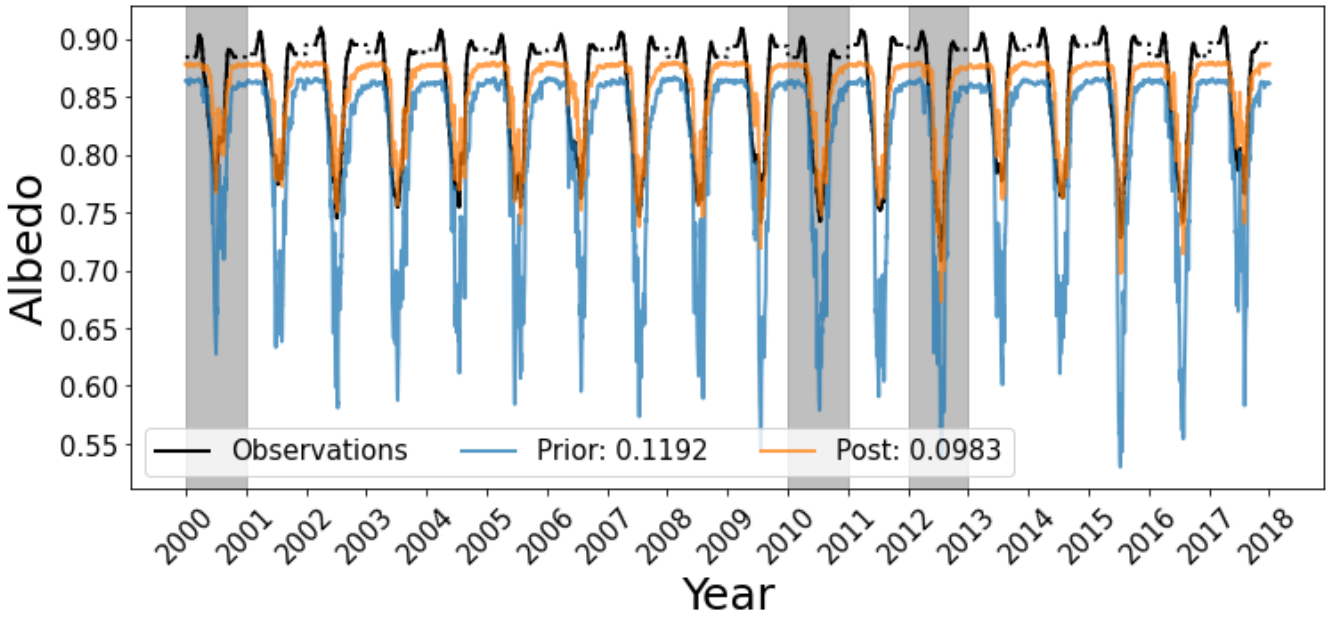

b)

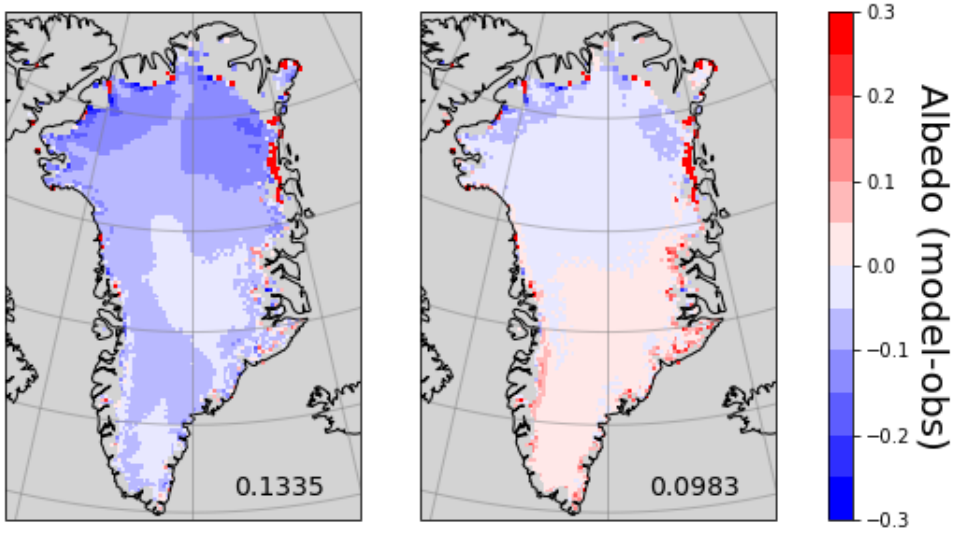

Figure 4. a) Time series of the albedo (averaged over space). The retrieved values (black), prior simulation (blue), and posterior simulation, i.e. using the optimal parameter set, (orange) are shown. The values in the legend denote the RMSD between each simulation and the retrieved albedo. b) Spatial distribution of differences between the model and the retrieved albedo averaged over March-October for the years 2000-2017 for both the prior (left) and posterior (right) models, with the total RMSD in the bottom right-hand corner.

Table 2. Percentage reduction in model-data RMSD between the prior and posterior runs over March-October. The years used in the optimisation are shown in bold.

	Whole area	Edges	Middle
2000	**22.3**	**11.27**	**37.62**
2001	25.73	11.22	43.36
2002	26.17	12.07	42.13
2003	28.89	12.39	44.65
2004	26.85	11.77	43.79
2005	27.08	9.38	45.36
2006	21.39	8.21	37.92
2007	26.55	6.49	46.06
2008	27.1	10.44	43.98
2009	29.17	11.75	45.61
2010	**27.21**	**8.41**	**46.15**
2011	27.31	6.65	46.46
2012	**25.76**	**7.02**	**42.3**
2013	25.0	6.54	43.61
2014	24.58	6.79	42.46
2015	27.35	10.19	43.09
2016	28.46	8.79	45.31
2017	26.04	11.7	41.9
ALL	26.37	9.52	43.68

also leads to a smaller decay term. Finally, we see that omega values increase and beta values decrease. By doing so, these two parameters increase the value of g_{temp} which appears in the denominator of f_{age} (Eq. 3) hence slowing down snow ageing.

We also notice some differences between the three sets of posterior parameters. Since the "Both" optimisation includes points from both of the other optimisations, we might expect the posterior parameters to be in between the "Edges" and "Middle" posterior parameter values acting as a compromise between both optimisations. However, this is only true for two out of the eight parameters. Instead, the "Both" posterior parameters often take higher or lower values than parameters from the other two optimisations. This behaviour suggests that parameter space is not smooth but full of local minima (this supports the results from Sect. A, where the gradient-based algorithm struggled to improve the cost function). The clearest example of the "Both" optimisation performing differently is for the parameters δ_c and τ_{max}. These increase and decrease respectively for the "Edges" and "Middle" optimisations. However, for the "Both" optimisation, the opposite is true. These parameters can be highly anti-correlated (Fig. 6b). If δ_c is very small, the snow's age does not reset to zero, so the snow ages for longer, necessitating a larger value of τ_{max}. Therefore, these two parameters compensate for each other.

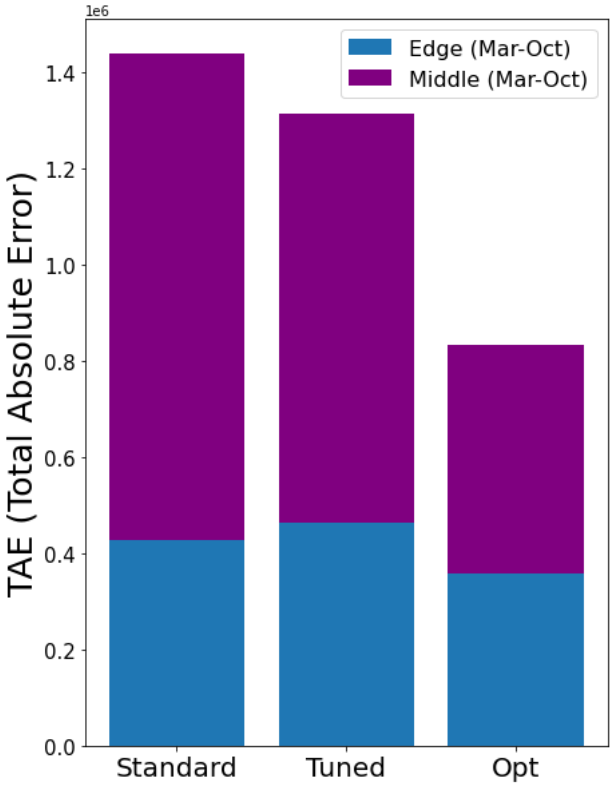

Figure 5. Total Absolute Error between the modelled and the retrieved MODIS albedo for the standard ORCHIDEE (i.e., default parameters values, left), the manually tuned (middle), and the optimised (i.e., using Bayesian framework, right) models. The Total Absolute Error is decomposed in each case, illustrating the contribution of the edge and middle points to the error for March-October.

4 Impact of the different parameter set on modelling the surface mass balance of the Greenland Ice Sheet

In Fig. 7 and 8, we consider how the different parameter sets discussed in this study impact the modelled snow states. To assess the performance of the different ORCHIDEE parameter sets, we compare the model outputs to that of the MAR model. Although MAR is a model with its own biases and errors, it has been shown to have good estimations of the different snow states (Fettweis et al., 2017, 2020) and so is a good product against which to compare.

In particular, we are interested in better modelling the surface mass balance (SMB). It measures the difference between mass gains and ablation processes, hence dominating the rates of mass change over the GrIS. Compared to MAR, the manually tuned version of ORCHIDEE performs best at simulating SMB. This can be seen both spatially and temporally. Spatially, the differences between MAR and the ORCHIDEE simulations are observed at the edges - especially in the north and west of the GrIS. The most noticeable difference in the ORCHIDEE runs can be seen at the west of the ice sheet, where the tuned model simulates SMB the best when compared to MAR, followed by the optimised model. In both the manually tuned and optimised models, the SMB is reduced at the west of the ice sheet compared to the default ORCHIDEE model. This is mirrored

a)

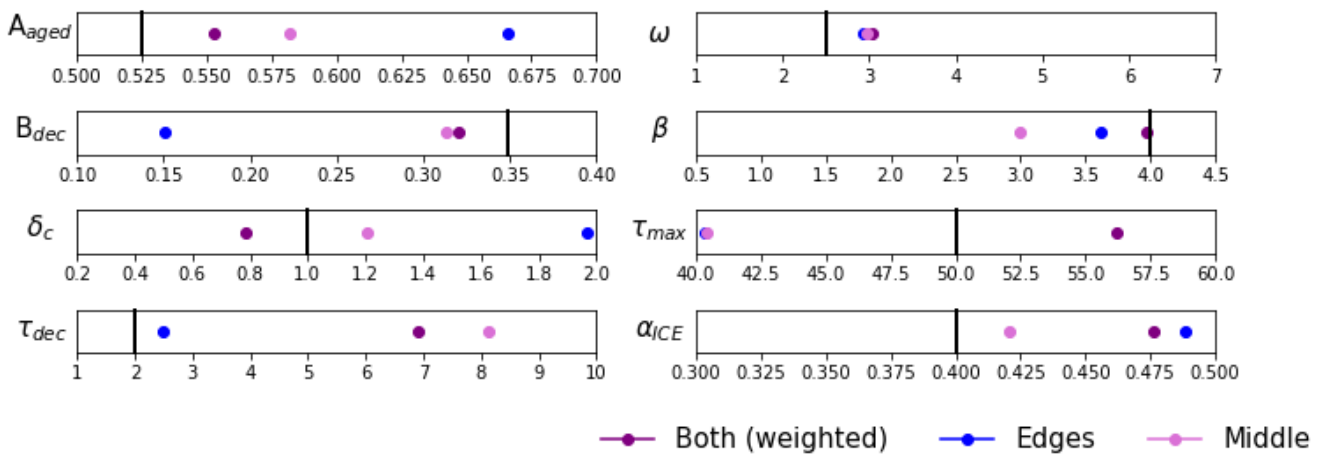

b)

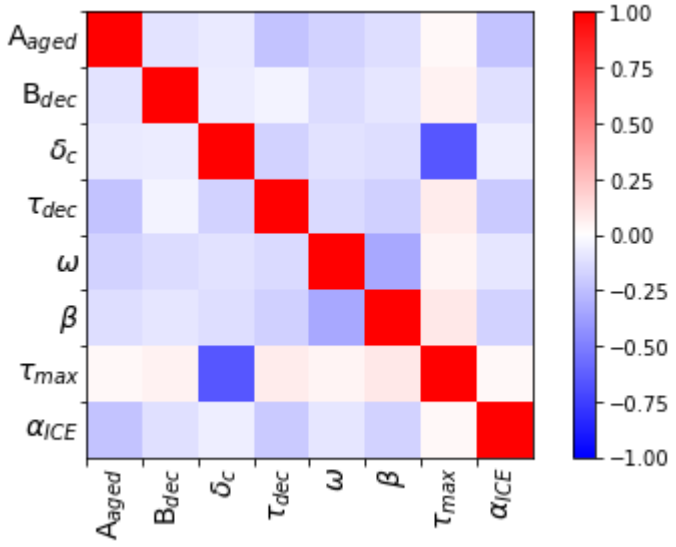

Figure 6. a) Posterior parameter values found for three different optimisations; "Both" where the middle and edge points are weighted with a ratio of 1:4, "Edges" where only the edge points were used in the optimisation, and "Middles" where only the middle points were used. Each box's range represents the variation used for each parameter during the optimisation. The vertical black line represents the prior parameter value. b) Correlations between the posterior parameters calculated at the optimum of the "Both" optimisation.

by an increase in runoff at the west of the ice sheet. Indeed, for simulated runoff, changes are mainly found at the west of the ice sheet, with the tuned model performing the best and the optimised model second when compared to MAR. Both models improve the fit compared to the default ORCHIDEE simulations. However, neither model is able to capture the magnitude of the runoff in summer, with the tuned model still only simulating half the expected magnitude of runoff.

When we consider modelled sublimation, we get the most different results. By increasing the albedo over the ice sheet, we decrease latent heat over the area and hence sublimation. When considering the time series, we see that the optimised model gets the correct magnitude of sublimation during the summer months. All of the ORCHIDEE simulations have a delayed peak compared to MAR and no sublimation is simulated by ORCHIDEE outside the summer months. When averaged over time, we see that MAR has high sublimation rates to the east of the GrIS. However, none of the ORCHIDEE simulations capture this. Instead, the sublimation over the centre of the ice sheet is what changes with the different parameter sets - with the optimised model lowering the rates the most. The strong impact that changing albedo has on simulated sublimation over the whole of the GrIS shows how coupled they are in the model.

Overall, with the optimised model, we do better than the standard ORCHIDEE model but not as well as the tuned model. During the manual tuning of the albedo parameters, the performance of the new parameters was assessed against several model outputs, including SMB, sublimation and runoff at each step of the trial and error procedure. We can think of this manual tuning as a multi-objective calibration. When performing the Bayesian optimisation, we get the best fit to the albedo. However, we overfitted to albedo with no other data, degrading the fit to other model outputs. As seen with the BFGS algorithm and the posterior parameters, parameter space is not smooth but has many local minima. As such, it is possible that a different solution exists, reducing the albedo to a similar extent whilst also improving the fit to other modelled outputs. To achieve this, we need to include more data in the optimisation to perform a multi-objective optimisation. If we cannot find such a parameter set, this would point to structural problems in the model, i.e., missing processes.

5 Discussion and conclusions

We have shown that by giving extra weight to the edge points during the optimisation, we can find a set of parameters that improves model-data fit for all the GrIS. The reduction of RMSD at the edges was similar to the reduction found when only focusing on the edge points during the optimisation. However, by including the middle points in the optimisation, the whole ice sheet greatly improved its fit to retrieved albedo. The model was optimised against three separate years simultaneously and validated against the rest of the time series. Improvements were consistent over all the years considered.

Parameter optimisation is a valuable tool for model development. Not only can it be used to find the best set of parameters for a given parameterisation, but more importantly, it can help identify structural issues in the model. When we cannot further improve the model against the observations, this can point to structural deficiencies in the model. For example, we cannot capture the different albedos in the north and south of the ice sheet with the current processes represented. More structural changes may help capture this variability. For example, we could look at further improving the snow/ice transfer processes by better discretising vertically the snowpack (Charbit et al., in prep.). Since we are running the ORCHIDEE offline - i.e.,

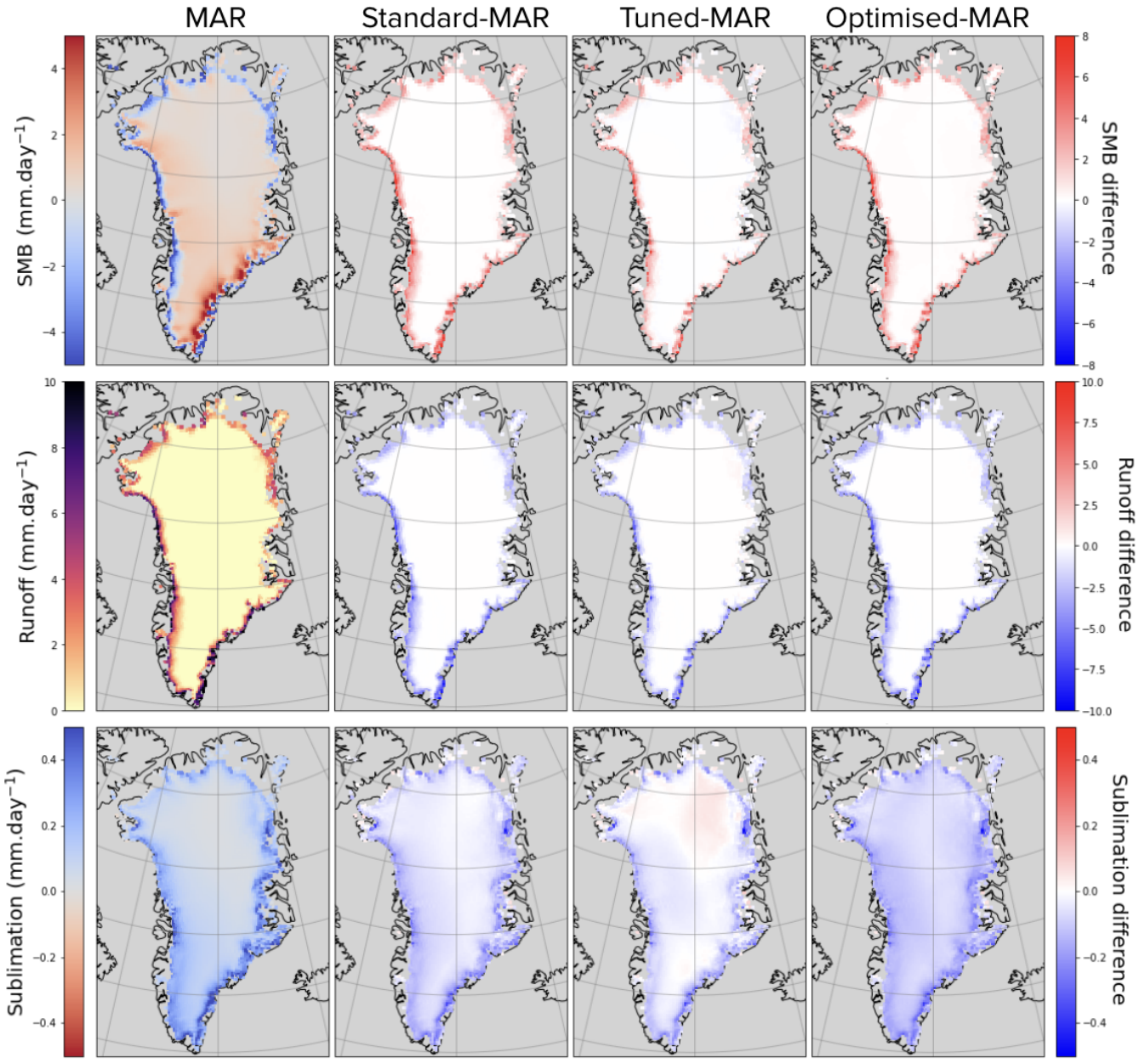

Figure 7. Impact of different parameter sets on ORCHIDEE simulations; "Standard" uses default parameter values, "Tuned" uses parameter values from the manual tuning and "Optimised" from the ORCHIDAS optimisation. Shown are spatial maps averaged over time (March-October) for MAR (left) and the difference between ORCHIDEE and MAR. Each row features a different variable of interest (Top: SMB, Middle: Runoff, Bottom: Sublimation).

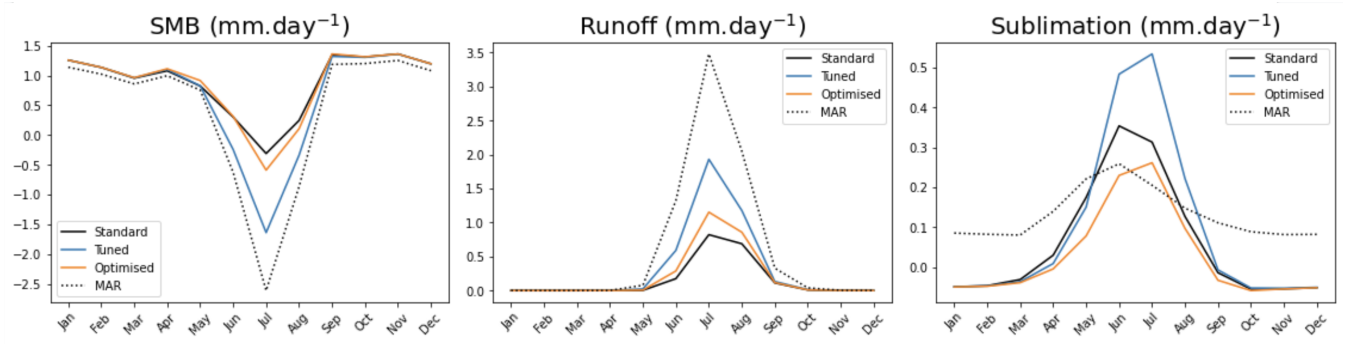

Figure 8. Same as Fig. 7 but showing monthly means averaged over space. This time the columns feature the different variables of interest.

prescribing the meteorological forcing - it would also be beneficial to run the model with different forcings to separate model structural errors from the errors in the forcing. This is important since MAR is a modelled estimate and, therefore, will be subject to its own biases and errors. We would want to ensure that we are correcting errors in the land surface model and not correcting atmospheric biases in the forcing data.

We must also remember that there are errors linked to the retrievals themselves. Indeed, the large uncertainties in the winter months led us to omit them for this study. For the other months, we set the observation errors to be the mean-squared difference between the observations and the prior model simulation to also account for the structural model errors. However, in practice, the true errors may be very different. For example, although steps to correct the solar zenith angle bias in the product have been undertaken, it is possible that the strength of the north-south albedo gradient observed in the data is an artefact of the product. Without clear and robust uncertainty quantification, we cannot disentangle natural GrIS processes from biases in the retrievals. There is an urgent need for data producers to provide this uncertainty, ideally at each time step. We further evaluate the optimisations with data from the same source, which will have the same systematic errors. One method to bypass this issue would be to evaluate the model using data from a different source, e.g., in situ data from the PROMICE network (Fausto et al., 2021). However, with these in situ data, we lack accurate local forcing data with which to drive the model, rendering such tests futile. One solution would be to run the model over these in situ sites with the same MAR atmospheric forcing at 20 km, but this then would lead to issues of scale and representativity. For additional evaluation, we are testing the application of this model and parameters to other polar and non-polar regions, starting with other ice sheets such as Antarctica.

In our optimisations, we put great importance on the edge points. However, these are also the points where we are most likely to find bare soil and vegetation instead of ice. These points could be represented by some of the other plant functional types in the model, which have different parameter values for A_{aged} and B_{dec}. To identify and separate these pixels from the ice-covered pixels used in this study, future experiments could exploit the ESA CCI (European Space Agency Climate Change Initiative) land cover product (ESA, 2017) allowing us to optimise these parameters for each of the plant functional types present.

We have also shown that while significantly improving the model's fit to retrieved albedo measurements, changing the parameters also influences the other model outputs. This was first done by performing a Morris sensitivity analysis. Morris was chosen since it only required a small number of model runs. However, its main limitation is that the sensitivity measure is only qualitative - the parameters are only ranked in order of significance but we do not quantify their absolute contribution. Furthermore, with this method, it is not possible to distinguish nonlinearity from interactions. It is also very dependent on the range of variations assigned to the parameters. Nevertheless, the Morris approach can still help give a broad overview of the most influential parameters and the model outputs they impact. We also showed the influence of the parameters on other model outputs by comparing simulated snow states to the MAR model. The optimised model was found to perform better than the original ORCHIDEE model but not as well as the tuned model for simulating SMB and runoff. For sublimation, the optimised model simulated the most accurate magnitude in summer; however, it still showed a bias when considered spatially.

Therefore, in addition to considering further structural changes, it will be necessary to further optimise the model against a range of datasets. With the ever-growing quantity of satellite datasets available, there are many different avenues we could consider. For example, we could use data from the GRACE (Gravity Recovery and Climate Experiment) satellite mission to constrain SMB (Sasgen et al., 2020). To constrain ice velocity, we could use products based on Sentinel-1 retrievals (Mouginot et al., 2017; Andersen et al., 2020) and data from the ESA CCI land surface temperature project (Karagali et al., 2022) could be used to constrain surface temperatures. Combining these datasets with MODIS albedo would result in a rich data source with which to optimise the model and learn about different processes governing the ice sheet.

Code availability. The ORCHIDEE vAR6 model code and documentation are publicly available via the ORCHIDEE wiki page (http://forge.ipsl.jussieu.fr/orchidee/browser/) under the CeCILL license (http://www.cecill.info/index.en.html, CeCILL, 2020). The associated ORCHIEE documentation can be found at https://forge.ipsl.jussieu.fr/orchidee/wiki/Documentation. The ORCHIDEE model code is written in Fortran90 and is maintained and developed under an SVN version control system at the Institute Pierre Simon Laplace (IPSL) in France. The ORCHIDAS data assimilation scheme (in Python) is available through a dedicated web site (https://orchidas.lsce.ipsl.fr).

Appendix A: Preliminary optimisations

Two preliminary optimisations were performed to select the minimisation algorithm (Sect. A), and a further experiment focusing solely on the edges of the ice sheet was undertaken in Sect. 3.3. These three test experiments were performed over the year 2000 (with the years 1998-1999 as spin-up).

A1 Algorithm choice

To choose which optimisation algorithm to use in the main experiment, we performed two preliminary tests optimising over a single year and over the whole of the GrIS (without weighting the edges). The results in Fig. A1 show the changes in the simulated albedo when averaged spatially. When using the L-BFGS-B algorithm, the improvement in model-data is indistin-

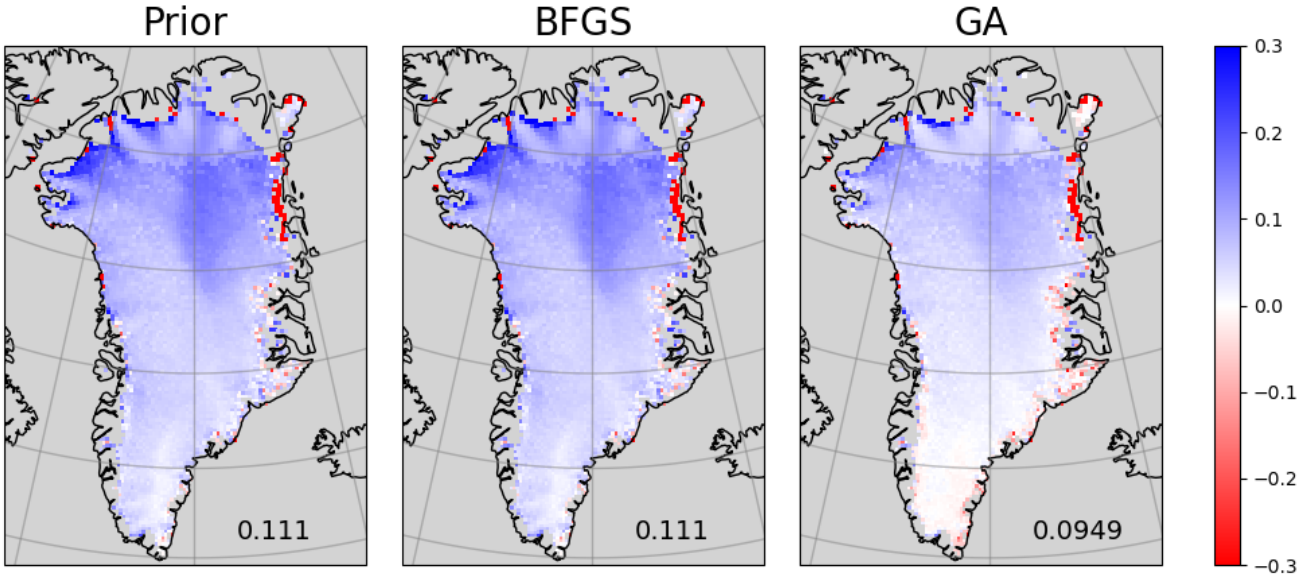

Figure A1. The differences between simulated and retrieved albedo over Greenland (averaged over March-October). Shown are the differences between the model and MODIS using its prior parameter values (left), parameters using the BFGS algorithm (middle), and parameters found using the GA algorithm (right). In each panel, the RMSD between MODIS and the different ORCHIDEE model versions is shown.

guishable (Fig. A1). Since the prior model used was already extensively manually tuned, it is likely that we started very near to a minimum (i.e., somewhere where the gradient is close to zero surrounded by positive gradient values). However, this is not the global minimum since we have been able to reduce the cost function further when using a different algorithm (i.e., in the GA case). Since gradient-based algorithms rely on negative gradient values to minimise the cost function, the gradient-based algorithm is unable to leave local minima, and therefore, the cost function is hardly minimised. In comparison, with GA, the RMSD is reduced by over 10% (Fig. A1). This improvement can be seen over most of the GrIS and most notably in the south of the ice sheet. The north is still underestimated, but to a lesser extent than with the prior model.

A2 Weighting the edge of the ice sheet

To see what the maximal improvement in model-data fit we can expect over these edges, we performed a preliminary experiment optimising only these points and only over the months March-October (Table 2). We were able to reduce the RMSD at these points by approximately 10%. This optimisation was also able overall to improve the simulated albedo in the middle of the ice sheet in summer. This implies there is some consistency between the edge and middle points for the 2000 - 2017 period. However, this optimisation did not improve the middle points consistently - for example, we observe a degradation in fit for the year 2000. It also degrades the fit of albedo in the winter months; the maximum albedo value attained in winter was much

Table A1. Results of a preliminary experiment optimising only the edge points of the GrIS for March-October of 2000. The optimisation was performed using the GA algorithm. Percentage reduction of model-data RMSD. Negative numbers show an increase in RMSD i.e. a degradation in fit.

Year	Edge points	Middle points	All points
2000	11.86	-6.01	3.14
2000-2017	10.11	8.51	9.21

lower than the retrieved values. Although the winter values are more uncertain, they still give an idea of the maximal albedo over the GrIS after snow accumulation.

Appendix B: Parameter information

B1 Parameter values

Table B1. Parameters of the snow albedo model. Default values refer to parameters used in a standard ORCHIDEE simulation, tuned parameters refer to values found after the manual tuning experiments, and the optimised parameters refer to parameters values found after using ORCHIDAS.

Parameter	Description	Default	Manually tuned	Optimised
A_{aged}	Sum to be the albedo of fresh snow	0.62	0.525	0.553
B_{dec}		0.169	0.349	0.320
δ_c	Snowfall depth required to reset the snow age (m)	0.2	1	0.783
τ_{dec}	Snow age decay rate (days)	10	2	6.911
ω	Tuning constants for glaciated snow covered areas	7	2.5	3.037
β		4	4	3.974
τ_{max}	Maximum snow age	50	50	56.183
α_{ICE}	Ice albedo	0.4	0.4	0.476

B2 Additional parameters

To get a better overview of the model output sensitivities, we consider addition parameters used to calculate the local rate of density change in the i^{th} layer of the snowpack:

$$\frac{1}{\rho_{snow}(i)}\frac{\delta\rho_{snow}(i)}{\delta t} = \frac{g.\mathcal{M}(i)}{\eta(i)} + \psi(i) \tag{B1}$$

The first term, represents the compaction due to snow load. This depends on the pressure of the overlying snow, calculated using the gravitational constant (g; m.s^{-2}) and the cumulative snow mass ($\mathcal{M}$; kg.m^{-2}) and snow viscosity (η). The second

term describes the effect of metamorphism (ψ), which can also be thought of as determining the settling of freshly fallen snow since this effect is most significant for newly fallen snow. Both the snow viscosity (η) and settling of freshly fallen snow (ψ) are solved in ORCHIDEE using the following empirical exponential functions of snow density (ρ_{snow}) and temperature (T_{snow}):

$$\eta(i) = \mathbf{v_0} \exp(\mathbf{v_1}(T_f - T_{snow}(i)) + \mathbf{v_2}\rho_{snow}(i)), \tag{B2}$$

$$\psi(i) = \mathbf{s_0} \exp(-\mathbf{a_1}(T_f - T_{snow}(i)) - \mathbf{s_2}(\max(0, \rho_{snow}(i) - \boldsymbol{\rho_d})). \tag{B3}$$

where T_f is the triple-point temperature for water. The rest are parameters whose values and ranges of variation used in the sensitivity analysis are outlined in Table B2.

Table B2. Parameters used to calculate the local rate of density change. The default value refers to the value used in a standard ORCHIDEE simulation, min and max refer to the ranges over which the parameters are allowed to vart during out experiments.

Equation	Parameter	Units	Default	Min	Max
η (Eq. B2)	v_0	Pa s	3.7 x 10^{-7}	1.5 x 10^{-7}	4 x 10^{-7}
	v_1	K^{-1}	0.081	0.08	0.35
	v_2	$m^3.kg^{-1}$	0.018	0.009	0.02
ψ (Eq. B3)	s_0	s^{-1}	2.8 x 10^{-6}	1.5 x 10^{-6}	3.5 x 10^{-6}
	s_1	K^{-1}	0.04	0.01	0.1
	s_2	$m^3.kg^{-1}$	460	320	600
	ρ_d	$km.m^{-3}$	150	100	200

Author contributions. SC and CD developed the snow model for its application over the GrIS, with support from FM and CO. VB developed the ORCHIDAS system and, with NR, expanded its application over 2D surfaces. NR integrated the sensitivity analyses to ORCHIDAS. Prior model tuning was performed by SC and CD. NR performed the optimisations and sensitivity experiments. NR generated the figures. All authors contributed to analysing the results, and writing the manuscript.

Competing interests. We declare that no competing interests are present.

Acknowledgements. Nina Raoult is funded by the European Space Agency (ESA) as part of the Climate Change Initiative (CCI) fellowship (ESA ESRIN/Contract No. 4000133601). We would like to thank the ORCHIDEE Project Team for developing and maintaining the ORCHIDEE code.

References

Andersen, J. K., Kusk, A., Boncori, J. P. M., Hvidberg, C. S., and Grinsted, A.: Improved ice velocity measurements with Sentinel-1 TOPS interferometry, Remote Sensing, 12, 2014, 2020.

Bamber, J. L., Griggs, J., Hurkmans, R., Dowdeswell, J., Gogineni, S., Howat, I., Mouginot, J., Paden, J., Palmer, S., Rignot, E., et al.: A new bed elevation dataset for Greenland, The Cryosphere, 7, 499–510, 2013.

Bastrikov, V., MacBean, N., Bacour, C., Santaren, D., Kuppel, S., and Peylin, P.: Land surface model parameter optimisation using in situ flux data: comparison of gradient-based versus random search algorithms (a case study using ORCHIDEE v1. 9.5. 2), Geoscientific Model Development, 11, 4739–4754, 2018.

Bonan, B., Nodet, M., Ritz, C., and Peyaud, V.: An ETKF approach for initial state and parameter estimation in ice sheet modelling, Nonlinear Processes in Geophysics, 21, 569–582, 2014.

Boucher, O., Servonnat, J., Albright, A. L., Aumont, O., Balkanski, Y., Bastrikov, V., Bekki, S., Bonnet, R., Bony, S., Bopp, L., et al.: Presentation and evaluation of the IPSL-CM6A-LR climate model, Journal of Advances in Modeling Earth Systems, 12, e2019MS002 010, 2020.

Box, J. E., Van As, D., and Steffen, K.: Greenland, Canadian and Icelandic land-ice albedo grids (2000–2016), GEUS Bulletin, 38, 53–56, 2017.

Byrd, R. H., Lu, P., Nocedal, J., and Zhu, C.: A limited memory algorithm for bound constrained optimization, SIAM Journal on scientific computing, 16, 1190–1208, 1995.

Campolongo, F., Cariboni, J., and Saltelli, A.: An effective screening design for sensitivity analysis of large models, Environmental modelling & software, 22, 1509–1518, 2007.

Carsel, R. F. and Parrish, R. S.: Developing joint probability distributions of soil water retention characteristics, Water resources research, 24, 755–769, 1988.

Charbit, S., Dumas, C., Maignan, F., Ottlé, C., and Raoult, N.: Adapting snowpack modelling to ice surfaces in the ORCHIDEE land surface model: Application to the Greenland ice sheet surface mass balance, in prep.

Cheruy, F., Ducharne, A., Hourdin, F., Musat, I., Vignon, É., Gastineau, G., Bastrikov, V., Vuichard, N., Diallo, B., Dufresne, J.-L., et al.: Improved near-surface continental climate in IPSL-CM6A-LR by combined evolutions of atmospheric and land surface physics, Journal of Advances in Modeling Earth Systems, 12, e2019MS002 005, 2020.

Cook, J. M., Tedstone, A. J., Williamson, C., McCutcheon, J., Hodson, A. J., Dayal, A., Skiles, M., Hofer, S., Bryant, R., McAree, O., et al.: Glacier algae accelerate melt rates on the south-western Greenland Ice Sheet, The Cryosphere, 14, 309–330, 2020.

Dantec-Nédélec, S., Ottlé, C., Wang, T., Guglielmo, F., Maignan, F., Delbart, N., Valdayskikh, V., Radchenko, T., Nekrasova, O., Zakharov, V., et al.: Testing the capability of ORCHIDEE land surface model to simulate A rctic ecosystems: Sensitivity analysis and site-level model calibration, Journal of Advances in Modeling Earth Systems, 9, 1212–1230, 2017.

Dee, D. P., Uppala, S. M., Simmons, A. J., Berrisford, P., Poli, P., Kobayashi, S., Andrae, U., Balmaseda, M., Balsamo, G., Bauer, d. P., et al.: The ERA-Interim reanalysis: Configuration and performance of the data assimilation system, Quarterly Journal of the royal meteorological society, 137, 553–597, 2011.

d'Orgeval, T., Polcher, J., and De Rosnay, P.: Sensitivity of the West African hydrological cycle in ORCHIDEE to infiltration processes, Hydrology and Earth System Sciences, 12, 1387–1401, 2008.

Ducharne, A.: The hydrol module of ORCHIDEE: Scientific documentation, 2016.

ESA: Land Cover CCI Product User Guide Version 2. Tech. Rep., Tech. rep., European Space Agency, Available at: maps.elie.ucl.ac.be/CCI/viewer/download/ESACCI-LC-Ph2-PUGv2_2.0.pdf, 2017.

Fausto, R. S., van As, D., Mankoff, K. D., Vandecrux, B., Citterio, M., Ahlstrøm, A. P., Andersen, S. B., Colgan, W., Karlsson, N. B., Kjeldsen, K. K., et al.: Programme for Monitoring of the Greenland Ice Sheet (PROMICE) automatic weather station data, Earth System Science Data, 13, 3819–3845, 2021.

Fettweis, X., Box, J. E., Agosta, C., Amory, C., Kittel, C., Lang, C., van As, D., Machguth, H., and Gallée, H.: Reconstructions of the 1900–2015 Greenland ice sheet surface mass balance using the regional climate MAR model, The Cryosphere, 11, 1015–1033, 2017.

Fettweis, X., Hofer, S., Krebs-Kanzow, U., Amory, C., Aoki, T., Berends, C. J., Born, A., Box, J. E., Delhasse, A., Fujita, K., Gierz, P., Goelzer, H., Hanna, E., Hashimoto, A., Huybrechts, P., Kapsch, M.-L., King, M. D., Kittel, C., Lang, C., Langen, P. L., Lenaerts, J. T. M., Liston, G. E., Lohmann, G., Mernild, S. H., Mikolajewicz, U., Modali, K., Mottram, R. H., Niwano, M., Noël, B., Ryan, J. C., Smith, A., Streffing, J., Tedesco, M., van de Berg, W. J., van den Broeke, M., van de Wal, R. S. W., van Kampenhout, L., Wilton, D., Wouters, B., Ziemen, F., and Zolles, T.: GrSMBMIP: intercomparison of the modelled 1980–2012 surface mass balance over the Greenland Ice Sheet, The Cryosphere, 14, 3935–3958, https://doi.org/10.5194/tc-14-3935-2020, 2020.

Fischer, G., Nachtergaele, F., Prieler, S., Van Velthuizen, H., Verelst, L., and Wiberg, D.: Global agro-ecological zones assessment for agriculture (GAEZ 2008), IIASA, Laxenburg, Austria and FAO, Rome, Italy, 10, 2008.

Frederikse, T., Buchanan, M. K., Lambert, E., Kopp, R. E., Oppenheimer, M., Rasmussen, D., and van de Wal, R. S.: Antarctic Ice Sheet and emission scenario controls on 21st-century extreme sea-level changes, Nature communications, 11, 1–11, 2020.

Gallée, H. and Schayes, G.: Development of a three-dimensional meso-γ primitive equation model: katabatic winds simulation in the area of Terra Nova Bay, Antarctica, Monthly Weather Review, 122, 671–685, 1994.

Goldberg, D.: Genetic Algorithms in Search, Optimization and Machine Learning, Addison-Wesley, 1989.

Hall, D. and Riggs, G.: MODIS/Terra Snow Cover Daily L3 Global 500m Grid, Version 6. Greenland coverage., National Snow and Ice Data Center, NASA Distributed Active Archive Center, Boulder, Colorado USA., http://nsidc.org/data/MOD10A1/versions/6, accessed December 2016., 2016.

Hall, D. K., Riggs, G. A., and Salomonson, V. V.: Development of methods for mapping global snow cover using moderate resolution imaging spectroradiometer data, Remote sensing of Environment, 54, 127–140, 1995.

Haupt, R. L. and Haupt, S. E.: Practical genetic algorithms, John Wiley & Sons, 2004.

Hu, A., Meehl, G. A., Han, W., and Yin, J.: Effect of the potential melting of the Greenland Ice Sheet on the Meridional Overturning Circulation and global climate in the future, Deep Sea Research Part II: Topical Studies in Oceanography, 58, 1914–1926, 2011.

Karagali, I., Barfod Suhr, M., Mottram, R., Nielsen-Englyst, P., Dybkjær, G., Ghent, D., and Høyer, J. L.: A new L4 multi-sensor ice surface temperature product for the Greenland Ice Sheet, The Cryosphere Discussions, pp. 1–26, 2022.

Krinner, G., Viovy, N., de Noblet-Ducoudré, N., Ogée, J., Polcher, J., Friedlingstein, P., Ciais, P., Sitch, S., and Prentice, I. C.: A dynamic global vegetation model for studies of the coupled atmosphere-biosphere system, Global Biogeochemical Cycles, 19, 2005.

Kumar, S., Mocko, D., Vuyovich, C., and Peters-Lidard, C.: Impact of surface albedo assimilation on snow estimation, Remote Sensing, 12, 645, 2020.

Kuppel, S., Peylin, P., Chevallier, F., Bacour, C., Maignan, F., and Richardson, A.: Constraining a global ecosystem model with multi-site eddy-covariance data, Biogeosciences, 9, 3757–3776, 2012.

Malik, M. J., van der Velde, R., Vekerdy, Z., and Su, Z.: Assimilation of satellite-observed snow albedo in a land surface model, Journal of hydrometeorology, 13, 1119–1130, 2012.

Morris, M. D.: Factorial sampling plans for preliminary computational experiments, Technometrics, 33, 161–174, 1991.

Mouginot, J., Rignot, E., Scheuchl, B., and Millan, R.: Comprehensive annual ice sheet velocity mapping using Landsat-8, Sentinel-1, and RADARSAT-2 data, Remote Sensing, 9, 364, 2017.

Navari, M., Margulis, S. A., Tedesco, M., Fettweis, X., and Alexander, P. M.: Improving Greenland Surface Mass Balance Estimates Through the Assimilation of MODIS Albedo: A Case Study Along the K-Transect, Geophysical Research Letters, 45, 6549–6556, 2018.

NOAA: National Geophysical Data Center, 2-minute Gridded Global Relief Data (ETOPO2) v2, Tech. rep., NOAA National Centers for Environmental Information, https://doi.org/10.7289/V5J1012Q, 2006.

Qu, X. and Hall, A.: On the persistent spread in snow-albedo feedback, Climate dynamics, 42, 69–81, 2014.

Qu, Y., Liang, S., Liu, Q., He, T., Liu, S., and Li, X.: Mapping surface broadband albedo from satellite observations: A review of literatures on algorithms and products, Remote Sensing, 7, 990–1020, 2015.

Raoult, N. M., Jupp, T. E., Cox, P. M., and Luke, C. M.: Land-surface parameter optimisation using data assimilation techniques: the adJULES system V1. 0, Geoscientific Model Development, 9, 2833–2852, 2016.

Riggs, G. A., Hall, D. K., Román, M. O., et al.: MODIS snow products collection 6 user guide, National Snow and Ice Data Center: Boulder, CO, USA, 66, 2015.

Sasgen, I., Wouters, B., Gardner, A. S., King, M. D., Tedesco, M., Landerer, F. W., Dahle, C., Save, H., and Fettweis, X.: Return to rapid ice loss in Greenland and record loss in 2019 detected by the GRACE-FO satellites, Communications Earth & Environment, 1, 1–8, 2020.

Schaaf, C. B., Gao, F., Strahler, A. H., Lucht, W., Li, X., Tsang, T., Strugnell, N. C., Zhang, X., Jin, Y., Muller, J.-P., et al.: First operational BRDF, albedo nadir reflectance products from MODIS, Remote sensing of Environment, 83, 135–148, 2002.

Sobol, I. M.: Global sensitivity indices for nonlinear mathematical models and their Monte Carlo estimates, Mathematics and computers in simulation, 55, 271–280, 2001.

Tarantola, A.: Inverse problem theory and methods for model parameter estimation, SIAM, 2005.

Tedesco, M., Doherty, S., Fettweis, X., Alexander, P., Jeyaratnam, J., and Stroeve, J.: The darkening of the Greenland ice sheet: trends, drivers, and projections (1981–2100), The Cryosphere, 10, 477–496, 2016.

Thackeray, C. W., Hall, A., Zelinka, M. D., and Fletcher, C. G.: Assessing prior emergent constraints on surface albedo feedback in CMIP6, Journal of Climate, 34, 3889–3905, 2021.

The IMBIE team: Mass balance of the Greenland Ice Sheet from 1992 to 2018, Nature, 579, 233–239, 2020.

Toure, A. M., Reichle, R. H., Forman, B. A., Getirana, A., and De Lannoy, G. J.: Assimilation of MODIS snow cover fraction observations into the NASA catchment land surface model, Remote sensing, 10, 316, 2018.

Wang, T., Ottle, C., Boone, A., Ciais, P., Brun, E., Morin, S., Krinner, G., Piao, S., and Peng, S.: Evaluation of an improved intermediate complexity snow scheme in the ORCHIDEE land surface model, Journal of Geophysical Research: Atmospheres, 118, 6064–6079, 2013.

Xu, J. and Shu, H.: Assimilating MODIS-based albedo and snow cover fraction into the Common Land Model to improve snow depth simulation with direct insertion and deterministic ensemble Kalman filter methods, Journal of Geophysical Research: Atmospheres, 119, 10–684, 2014.

Xue, Y., Houser, P. R., Maggioni, V., Mei, Y., Kumar, S. V., and Yoon, Y.: Assimilation of satellite-based snow cover and freeze/thaw observations over high mountain Asia, Frontiers in earth science, 7, 115, 2019.

Zeitz, M., Reese, R., Beckmann, J., Krebs-Kanzow, U., and Winkelmann, R.: Impact of the melt–albedo feedback on the future evolution of the Greenland Ice Sheet with PISM-dEBM-simple, The Cryosphere, 15, 5739–5764, 2021.